Laser-plasma accelerators and detectors for a compact monoenergetic Thomson Photon Source

C.G.R. Geddes[1,a], N.H. Matlis[1], S. Steinke[1], E. Esarey[1], D.E. Mittelberger[1,2], S. Rykovanov[1,3], C.B. Schroeder[1], Cs. Toth[1], K. Nakamura[1], J.-L Vay[1], B. Ludewigt[1], B.J. Quiter[1], P. Barton[1], Y. Zhang[1,2], K. Vetter[1,2], W.P. Leemans[1, 2]

[1] Lawrence Berkeley National Laboratory, 1 Cyclotron Road, Berkeley CA 94720.

[2] also at: U.C. Berkeley. [3] now at: Helmholtz Institute Jena.

[a] Corresponding author: cgrgeddes@lbl.gov

Laser-driven plasma based electron accelerators (LPAs) [1] have potential to enable future transportable narrow energy spread MeV photon (gamma ray) sources based on Thomson scattering [2]. Such sources could improve sensitivity at greatly reduced dose for applications using Nuclear Resonance Fluorescence [3,4], radiography [5], and photofission [6] based SNM detection and in related areas such as fuel characterization. The ability to select energy, energy spread, flux, and pulse structure to deliver only the photons needed can resolve many of the issues with current broad-band photon sources, including unnecessary dose that can interfere with the signatures to be detected and/or restrict operations [7]. MPS applications have however been limited by the sizes of the required high-energy electron accelerator, scattering laser, and electron beam dump.

This report summarizes results of a three-year project at the BELLA Center of LBNL which addressed needs for a compact Thomson photon source based on LPAs, and developed LPAs with the required beam quality. Simulations of laser-plasma accelerators and scattering to produce photons are summarized in Section 1, resulting in design of an LPA based photon source. The source will produce intense, pulsed photon beams which are a challenge for conventional detectors. Photon detector techniques suitable for such beams are described in Section 2. Experiments were conducted under the project to establish that LPAs can produce suitable beam quality for a photon source. As described in Section 3, this included control of the accelerator structure to reduce the size of the required drive laser, control of injection to reduce energy spread, and demonstration of emittance (focusability) comparable to state of the art conventional linacs. The project also developed techniques for plasma beam disposal to reduce background radiation and shielding needs, as presented in Section 4. Taken together, these project results support the feasibility of a compact LPA based Thomson photon source (concept: Figure 1). The source would combine a dedicated laser, cm-scale LPA accelerator, scattering, and detectors. Plasma based beam deceleration and disposal would help reduce shielding requirements. This report summarizes and includes references to project publications, referenced as [AuthorYYYY]. References to select background literature articles, referenced as [Number] are listed separately. Project publications contain in depth references to the general literature in the field, not all of which are reproduced here.

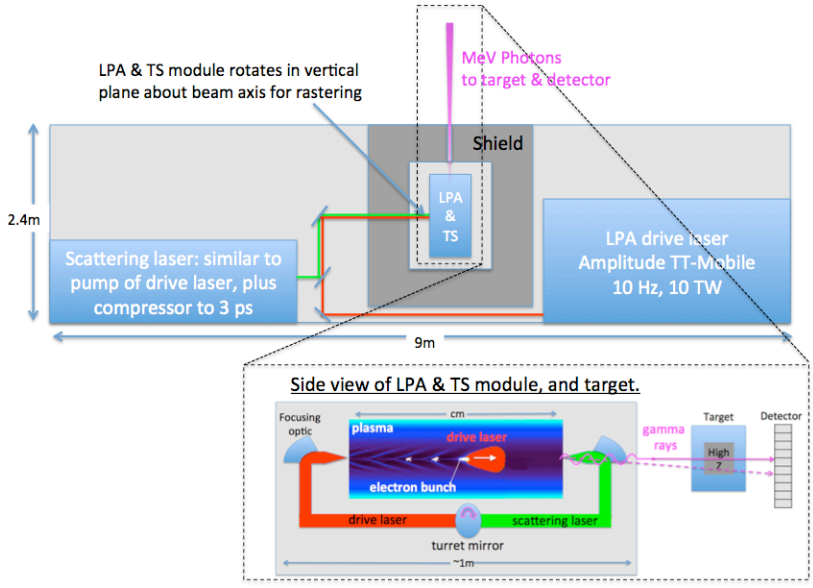

Figure 1. A conceptual LPA source based on state of the art lasers could be packaged in an intermodal container. Top image is the overall layout. Lower image is a side view of the LPA and Thomson scattering module and the resulting photon beam and target. An LPA drive laser at the 10 TW level is suitable for 1-2 MeV photons. Lasers are rapidly developing, including kHz systems as needed for applications, and these new systems are also anticipated to be more compact than illustrated here.

1. *Accelerator and Thomson scattering photon source simulations and design*

Simulations of LPA-based Thomson photon sources (Figure 2), of plasma beam deceleration/disposal to avoid unwanted background radiation, and of the LPA were conducted to improve accelerator performance and to inform future photon source design. Photon source simulations established parameters required from the accelerator to guide LPA development. They then designed both near term photon source experiments accessible using state of the art lasers, and concepts for future high flux and very narrow bandwidth sources. LPA simulations guided the experiments on laser guiding and injection control into the accelerator to improve performance towards the requirements of photon sources. In this report, simulations of deceleration are covered in section 4.

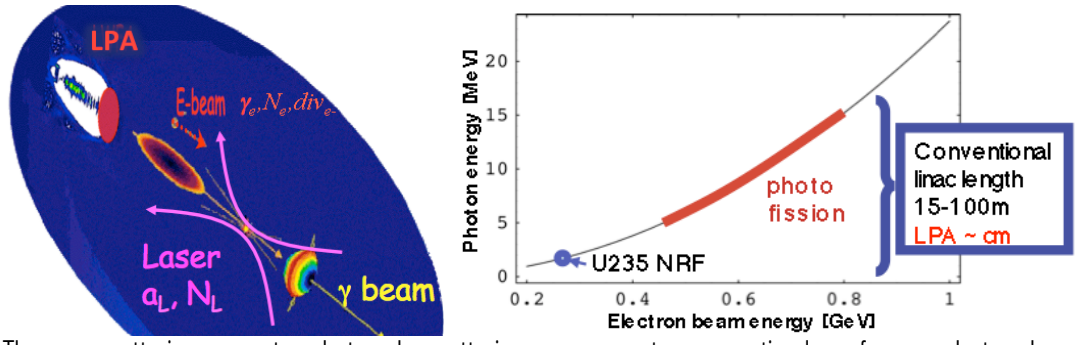

Figure 2. Thomson scattering generates photons by scattering a near-counterpropagating laser from an electron beam. Photon bandwidth is determined chiefly by electron beam energy spread and divergence provided laser intensity is low and pulse length long. The process requires high-energy electron beams, at the 200 – 800 MeV level, to generate MeV photons. This is in contrast to Bremsstrahlung sources which operate with lower electron energies, and motivates use of compact accelerators and beam disposal systems.

Thomson scattering of a laser from a counter-propagating electron beam is a well established source of quasi-monoenergetic photons, whose application is currently limited by the need for high-energy linacs and associated shielding, which are large fixed facilities using conventional technology. The energy E_{sc} of a photon near-backscattered by an electron at $\gamma_e \sim 2E_e$[MeV] is relativistically upshifted [8]:

$$E_{sc} = \frac{4\gamma_e^2}{1+\gamma_e^2\theta^2+a_0^2/2}E_L$$

with E_L the laser photon energy and q the scatter angle. Available high power lasers typically have $E_L \sim 1.5$ eV ($\lambda \sim 800$nm). Hence 200 MeV electrons are required for 1 MeV photons, and 600 MeV electrons for 9 MeV photons. Frequency conversion allows $E_L \sim 3$ eV ($\lambda \sim 400$ nm), doubling scattered energy to 2-18 MeV, but use of lasers much below this wavelength is limited by the scattering cross section issues described below. Angular dependence in E_{sc} means that for narrow bandwidth (BW) the source must be collimated to much less than the emission angle $\theta \sim 1/\gamma_e$. This collimation then transmits a fraction of the total photons approximately equal to BW. Hence narrower BW requires more scattering events to generate N photons within BW, e.g. one photon in 1% BW requires 100 total events. For an electron bunch [2], radiation adds incoherently due to the very short scattered wavelength, and the resulting collimated photon energy spread convolves electron angular spread and energy spread. The contribution of bandwidth in E_L can be kept small because long laser pulses are used for high photon yield.

Current MeV sources include HIGS at Duke [9] and TREX/MEGA-Ray at LLNL [10]. A new generation includes sources under construction at the Extreme Light Infrastructure project in Romania [11] [5] and the Japan Atomic Energy Agency [4], and proposed facilities at FNAL [12], SLAC [13], the Canadian Light Source, and BNL [14]. Thomson scattering is so predictable and well understood it is routinely used as a beam diagnostic on conventional machines such as the ALS linac at LBNL [15] (experiments by the LBNL division director), HIGS at Duke [9], Helmholtz Zentrum Dresden Rossendorf [16], and for non-accelerator diagnostics including work by the project PI [17]. Initial experiments have demonstrated Thomson scattering from LPAs [18] by placing a foil to back-reflect the drive laser onto the electron beam [19], or a laser split from the LPA driver [20], but so far have resulted in very broad photon bandwidth and limited yield due to insufficient electron beam quality and lack of independent scattering laser control.

Simulation tools were developed to allow rapid evaluation of photon source parameters. The VDSR radiation code developed [RykovanovAAC2012, ChenPRSTAB2013] includes Thomson and Compton scattering processes and can also include analytic models of LPA acceleration, focusing, and deceleration. We also implemented proper-time integration to increase efficiency and allow more rapid exploration of

parameters. These codes were supported by analytic approximation which allow quick approximations of the photon energy spread due to main contributors such as laser bandwidth and amplitude, and electron beam energy spread and divergence. These tools were used to develop designs for LPA based Thomson photon sources. The full results including references are published in [RykovanovAAC2012, ChenPRSTAB2013, RykovanovJPB2014], and are summarized here.

Simulations and supporting theory show the beams from compact LPAs, shown in Section 3, are sufficient to produce low energy spread MeV photon beams via Thomson scattering at relevant fluxes per shot (Figure 3). For LPA parameters, divergence is the dominant contribution when energy spread is controlled at the 1% level as demonstrated in Section 3. The native divergence present in the LPA allows photon sources for radiography with 20% energy spread and 2 mrad divergence without refocusing the electron beam. Refocusing to increase beam diameter from the 0.1µm typical in the plasma [PlateauPRL2012] to the 1 µm level (and hence decrease divergence) allows 2% level energy spread for NRF. This can be accomplished using conventional magnetic quadrupole lenses [30], but this requires meter-scale distances and may make it difficult to maintain the short electron bunch lengths needed for deceleration (see Section 4). For these reasons, plasma lens parameters were derived, as well as other alternate methods for divergence control. These can meet requirements for divergence control in cm-scale distances for compatibility with deceleration [RykovanovJPB2014].

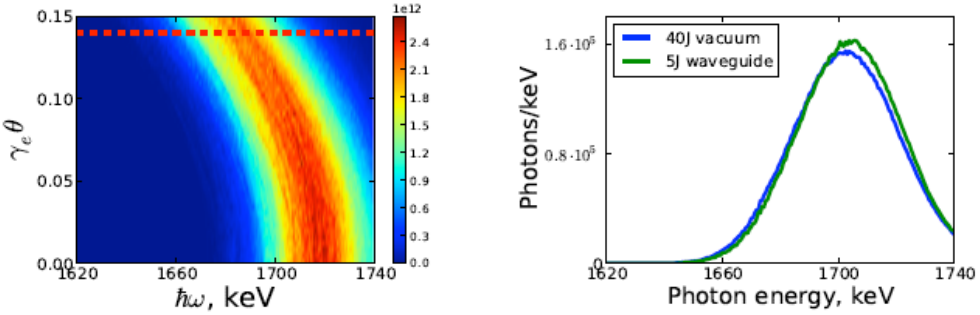

Figure 3. Simulated Thomson scattered energy-angle spectrum (left) and collimated spectrum (right) for a case using an LPA-like electron beam at 300 MeV, with energy spread similar to Figure 8 (left), and beam expansion to 1µm. Scattering produces a NRF relevant photon beam with energy spread (collimated at the red line) of 2%.

The simulations were used to define laser requirements and target area needs for experiments to validate production and control over the photon beam. The scattering laser must be independently controlled because the requirements for duration, pulse shape, chirp and other parameters are very different for high quality scattering than for LPA drive lasers . It must also be stable to meet needs to temporally synchronize and spatially overlap it to the LPA. Using state of the art LPAs demonstrated under the project (see Section 3), 1.7 MeV photons can be created with fluxes of ~10^7ph/s at 10 % bandwidth. Bandwidth and energy can be controlled via electron beam tuning, including up to 9 MeV photons (and 15 MeV if needed) from existing LPAs at 200-600MeV. Illustrative photon spectra simulated from realistic electron beam experimental conditions are shown in Figure 4.

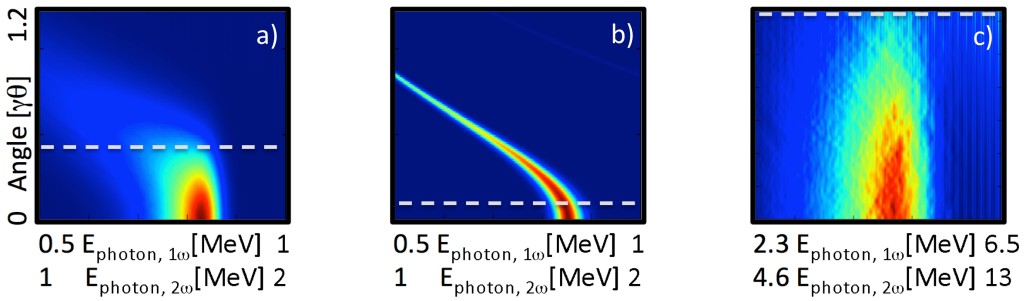

Figure 4. Photon spectra simulated for the electron beams of high quality LPAs (Section 3), and an independent scatter laser. (a) 200 MeV electron beams produce photon energy of 0.85 MeV with a scattering laser of 1ω (800nm), or 1.7 MeV with 2ω (400nm), both in 10% FWHM bandwidth set by beam divergence. (b) Few percent bandwidth could be produced by expanding the same electron beam to reduce its divergence. (c) 460 MeV electron beams produce 4.7 MeV or 9MeV photons using 800 nm or 400nm scattering lasers respectively, at bandwidth of 25% FWHM set by divergence. As above, beam expansion can reduce bandwidth. Collimator angles for each beam are illustrated with dashed lines

Due to the low scattering cross section and the need to keep scattering laser intensity low, the efficiency of scattering is a major driver of photon source size. To avoid unnecessarily high electron beam current (which increases accelerator size and power, and shielding size), scattering of order one photon per electron is desired, but this is challenging to achieve. There is a tradeoff between yield and bandwidth, and a realistic electron beam of 10^8 electrons can produce 10^8 photons with 10% energy spread, or ~10^7 with 2% energy spread. However, doing this conventionally requires a scattering laser energy much greater than that of the LPA driver, which dominates system size. This is because the laser spot size must be large to match its focal depth to the long laser pulse length required for narrow energy spread photon beams. Comparing to the equivalent quantity for 1 μm laser light, LPA electron beam emittance is three orders of magnitude smaller, and compensating this disparity is the key to obtaining efficient photon production. For interaction in vacuum, the emittance disparity means the electron beam will stay collimated over much longer distances than a laser pulse of equivalent spot size. For the low intensities typically required to limit nonlinear contributions to photon bandwidth, interaction distances at cm-scale are required to achieve ~1 photon per electron (as desired to obtain a given photon flux with minimal electron current and hence shielding). Focusing of the electron beam to spot sizes of ~ 1μm RMS is sufficient for this distance as well as to meet requirements for 1% level photon bandwidth. Typical laser spot sizes to obtain these focal depths are in contrast ≳15 μm, with all of the laser energy outside the electron beam radius being wasted. This is what drives the requirement for tens of joules of scattering laser energy. An insignificant fraction of the scattering laser photons are scattered (typically $<10^{-10}$), so depletion of its intensity is not a concern. Hence, there is no gain from increasing the electron beam spot size. Realizing high yield with the lower scattering laser energies needed for a compact source then requires that either the laser focal depth must be increased while keeping its radius small, or that the required interaction length must be shortened.

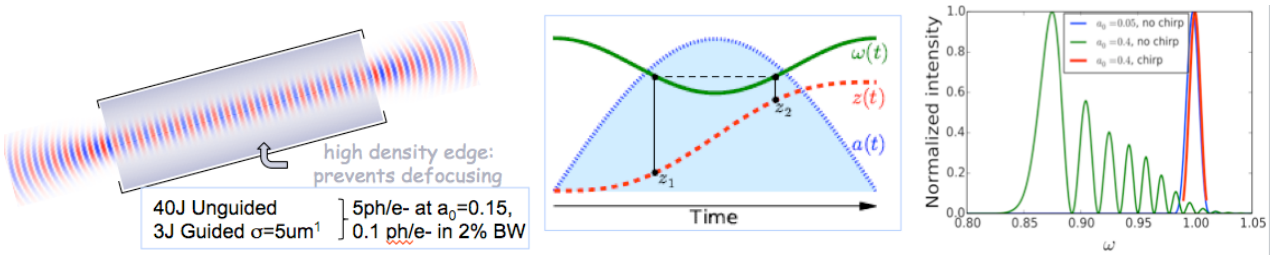

Figure 5. Controlled scattering could reduce the laser energy and electron current required to produce a given number of MeV photons. (Left) A plasma channel could guide the scattering laser, extending its focal depth and increasing photon yield. (center) Changing the laser frequency over time in a controlled way (chirp) could compensate nonlinear detuning of scattering. (right) This allows narrow bandwidth scattering at high intensity (a0), increasing photon yield.

The scattering laser focal depth can be extended by using a plasma channel (Figure 5). This technique has been used successfully in LPA experiments to guide the LPA drive laser over > 10 focal depths at guided spot sizes as small as 3 μm RMS [24]. These experiments used parabolic plasma density profiles with a minimum of density on axis, which forms a guiding fiber for the laser pulse that can withstand intensities beyond those required for Thomson scattering. Guiding the laser pulse even with a relatively relaxed waveguide at 6 micron RMS spot size would reduce the scattering laser energy from 40 J to 5 J at the same photon yield [RykovanovJPB2014]. A 3 μm spot size would allow energies approaching 1 J. For very narrow bandwidth photon sources, it may be desirable to use a nearly hollow plasma channel. This removes focusing forces on the electron beam while preserving laser focusing. Such channels are also of interest for high energy physics applications of LPAs where they can be used to control electron beam emittance [21]. Alternatively, increasing scattering laser intensity allows shorter interaction lengths while maintaining photon yield (Figure 5). Nonlinear detuning of scattered photon frequency has limited this approach: the high intensity peak of the laser profile scatters a different frequency than the low intensity wings. This nonlinear broadening can be compensated by designing a laser pulse with time-dependent frequency 'chirp' such that the change in frequency compensates for the nonlinear frequency shift at each time slice within the pulse [22]. An analytic model determining the parameters for such pulses were derived and submitted for publication. It requires controlled, broad bandwidth and chirp in the scattering laser. These approaches provide a path to producing high fluxes ≥ 1 photon/electron, reducing electron current, while using laser energy which is comparable to the LPA drive laser energy so as to mitigate both scattering laser and shielding contributions to MPS size. As described under Section 4, these simulations were integrated with deceleration simulations to design an all-in-

one compact plasma structure which accomplishes acceleration, high quality and efficient scattering, and deceleration of the electron beam.

Simulations, with community and user data, informed source needs and hence accelerator needs for active interrogation. Photon beams from the Thomson scattering simulations have been used as input for initial active interrogation simulations by collaborators. Quasi-monoenergetic beams improve sensitivity by eliminating photons outside the desired band, and reduce dose to enable operation in populated areas. Repetition rates at 1-10 kHz levels with 10^7 to 10^8 photons/shot satisfy scan rate and signal needs, while divergence of < 2 mrad allows cm-scale resolution in container scans, or stand off. Radiography penetrating 40 cm steel, and container scan rates of 80 cm/s at while penetrating 20 cm steel (ANSI standard) is accessible using 20% level energy spread, making this an attractive first application. Use of two or more energies provides Z discrimination. Photofission interrogation of a filled container or at 100m standoff benefits from 10% energy spread to avoid backgrounds. NRF is the most demanding: few-percent energy spreads near 1.7 MeV enable isotopic verification of a 2 cm object in a full container or fuel rod characterization. Since producing narrow energy spread requires tight control of electron beam and scattering, this requires most development. These limited simulations could be extended in future work to fully characterize the operation space and potential benefit of monoenergetic sources.

Colliding pulse and LPA simulations [CormierPRSTAB2014, ChenPRSTAB2013] guided experiments described in Section 3 and established scaling for a future photon source injector at NRF to photofission energies. They show that use of laser guiding and two-pulse colliding pulse controlled injection allows production of percent level energy spread at energies relevant to NRF sources from 10 TW class lasers. Photofission and radiography relevant energies are accessible using 40-100 TW. Beam charges of a few 10^8 electrons are achievable, consistent with desired photon fluxes. The results of these simulations were published.

Results show that state of the art lasers are sufficient for an experiment demonstrating the key elements of an LPA Thomson photon source, that compact LPAs can produce electron beams suitable for future high flux and high quality photon sources, and that associated plasma technologies of laser guiding and beam deceleration can resolve important non-accelerator issues which otherwise limit the source size. Such a source is accessible by upgrading the LBNL laser. Modern equipment is intrinsically more stable due to advanced manufacturing and controls, and also allows the entire system to fit in a single laser room adjacent to the experiment. This would provide the stability required to execute a source experiment, which our current laser does not provide. Fluxes of 10^{11}-10^{12}ph/s also require operation at kHz -10kHz repetition rates, which in turn requires laser development [23].

2. *High yield single shot MeV photon detectors*

A detector capable of measuring both the spatial and energy distributions of a high-yield single-shot of MeV-scale photons is important to development and to some uses of the photons produced by Thomson sources. Photons will be femtoseconds in duration and spaced ~1-100 micron apart, which is tighter than can conventionally be resolved, requiring new detectors. A realistic prototype was developed and tested to demonstrate suitability of a Compton scattering based technique for high yield photon detection.

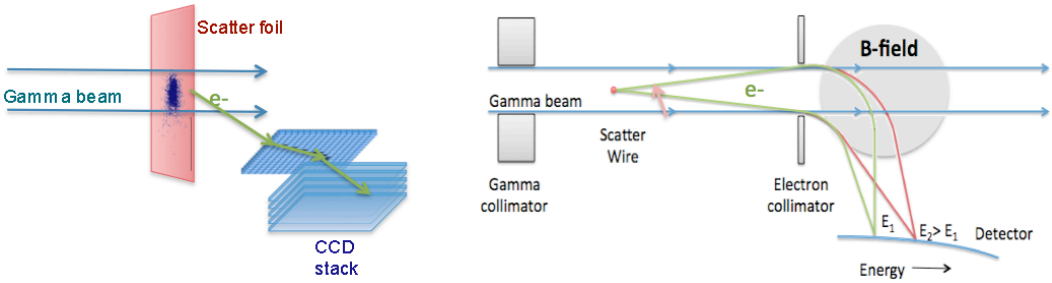

Figure 6. MeV photon detectors for energy angle spectra in single or few shots use Compton scattering of photons in a foil to generate electrons, which are characterized by a CCD (left) or spectrometer (right).

Detection concepts were developed that disperse the photon flux using Compton scattering in a foil placed in the photon beam, and analyze the scattered electrons (Figure 6). Sampling is to be accomplished by Compton scattering the photons off of electrons in a thin foil, which also effectively distributes scattered electrons over the surface of a pixelated detector. This distribution reduces the spatial flux density to levels that can be resolved. The origin (scattering) location of the electrons in the foil would then be estimated by back-

projection using the first several pixels from the imaged electron track. These first pixels produce a straight track before the random walk path takes over, terminating with a Bragg peak. With back projection determining scattering angle and the location on the foil where scattering occurred, the energy of the electron determines the energy of the photon incident on the scattering foil. The full energy of the Compton electron is to be measured with a stack of CCDs since the detection efficiency of silicon is relatively low at the 500-1500 keV electron energies which correspond to ~2 MeV photons. The key questions are then how accurately back projection and energy measurement can be achieved.

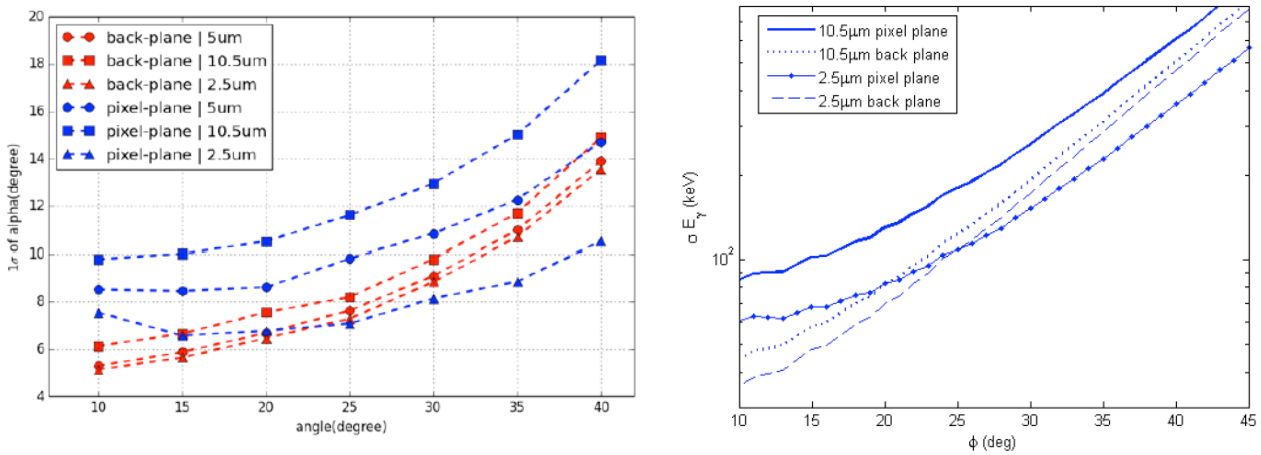

Figure 7. (left) Angular resolution as a function of scattering angle in the YZ plane for 1.8 MeV photons. (right) Energy resolution from Compton reconstruction due to angular uncertainty..

Simulation of Compton scattering based detection indicates that back projection using available CCDs is sufficient to provide ~5 resolution elements across the Thomson beam aperture. An example of such simulations, characterizing detector accuracy, is shown in Figure 7. This would be suitable to characterize sources of 5-10%-level energy spread for demonstration photon production experiments. Options for higher performance have also been considered. These include either smaller CCD pixel sizes or alternate detectors such as silicon pixel devices, silicon on insulator (SOI) CMOS devices, or a magnetic spectrometer.

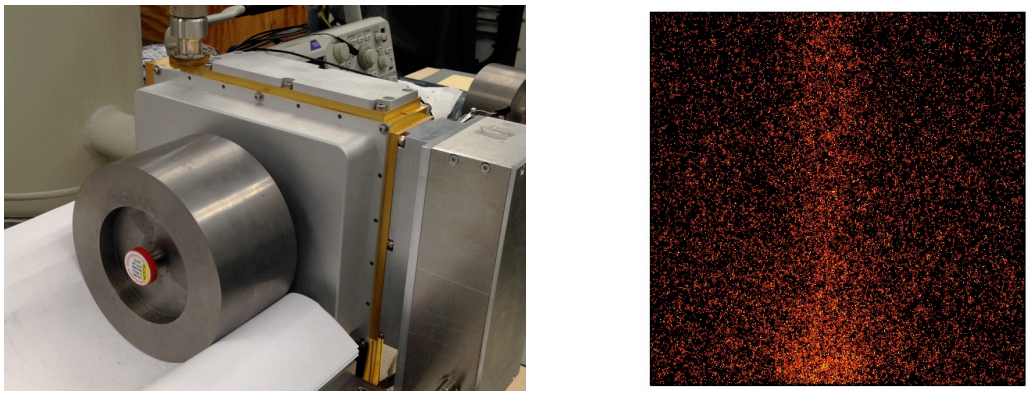

Figure 8. (left) 60Co source behind tungsten collimator aligned to Mylar window of vacuum cryostat, housing a 12 MPixel scientific CCD at 140 K. (right) The original 45,000 tracks from 30 images.

The detector prototype chosen to validate this scheme comprises: a 12 MPixel scientific CCD with 10.5 μm pixels and dimensions of 650 μm × 3.5 cm × 3.5 cm. The CCD is cooled to 140 K in a vacuum cryostat and held perpendicular to entrance (scattering) and exit windows made from 14 μm × 5 mm-diameter aluminized Mylar (Figure 8). The CCD subtends a significant solid angle for good sensitivity, and covers a range of Compton scattering angles which the simulations indicate could give good resolution. The CCD and scattering window are realistic prototypes of the systems which simulations indicate are appropriate, as described above. The low noise performance of the CCD also allowed multi-photon effects important to single shot detection to be tested by using long exposure times with an available radioactive source.

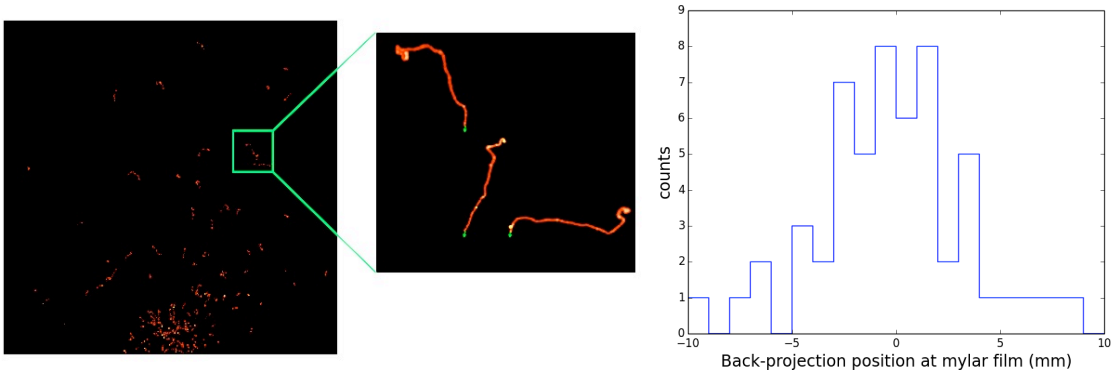

Figure 9. (left) Filtered image of tracks likely to have interacted in the Mylar window and zoom of three tracks pointing back to the window plane. (right) Back projection of 68 tracks at Mylar window plane.

The detection system was tested with a 0.15 mCi 60Co source with 1.17 MeV and 1.33 MeV photon energies. The source was placed at the back of a 3 mm-diameter tungsten collimator aligned to the scattering window of the cryostat. A sample of 30 images was taken, each with one minute exposure, yielding a total of 45,000 electron tracks. Most of these events are scattered photons within the collimator / cryostat and represent undesired (non-ROI) events that will not be present with the final 1.8 MeV beam. Rejection of these served as a test of the back projection algorithms. By applying appropriate cuts in energy, direction, track diffusivity and pileup, only a small number of events (68 events : 0.15%) remain (Figure 9). Their directions are back projected onto the Mylar film plane to obtain the spatial distribution of the beam. With more aggressive cuts, this method will provide sufficient spatial resolution for a burst of MeV-scale photons.

Other tests included installation of a pixel detector on the LPA beamline. This detector was run during LPA experiments, yielding experience with triggered, multi-photon operation. Triggering and resolution of multiple tracks were demonstrated synchronized to the LPA trigger which is a significantly different environment than typical for such radiation detectors. Similar experiments were conducted with scientific CCDs. The ability to synchronize and read out detectors with the LPA will be important for photon source experiments in the future.

Detector simulations and tests indicated the suitability of the developed concept to characterize the high flux photon beams anticipated from a Thomson source. The simulations also indicated paths to higher performance for future sources at percent level energy spread using higher resolution CCDs or magnetic spectrometers as detectors.

3: *Laser plasma accelerator injector development*

Improved electron beam quality from LPAs was realized through controlled electron injection using colliding laser pulses as well as through laser propagation/guiding control of the accelerator. LPAs produce the required 0.2-1 GeV electron energies for a Thomson photon source in ≤3 cm plasmas [1], allowing a total photon source length including laser focusing of ~1m. Required laser powers have however in the past been too high for mobile application, and electron beam quality has been insufficient to generate narrow energy spread Thomson photon beams. The experiments significantly improved performance, as needed for a photon source. The results were published in [PlateauPRL2012, MatlisAAC2012, GeddesAAC2014], and are summarized here.

The experiments were conducted on the 10 TW-class LOASIS laser system at the BELLA center of LBNL, which produces up to 0.6 J in 40 fs pulses at ≤ 10 Hz repetition rate. Previous to the present experiments, this system has produced electron beams via self trapping, including demonstration of few percent energy spread at 86 MeV through use of a preformed plasma channel to guide the drive laser, extending laser propagation length in the plasma [24]. Significant transverse leakage out of these preformed channels was observed. Electron beam energies without use of the channel were typically near 30 MeV, and plasma profiles and transmitted modes showed evidence of breakup of the laser pulse into multiple filaments, similar to results from other experiments. Previous attempts to control injection on this laser resulted in low energy beams [27]. This was attributed to the fact that the laser did not remain collimated through the plasma at the densities required.

Experiments showed that laser phase-front control via a deformable mirror can produce high quality laser focal spots over the full focal depth of the laser [MatlisAAC2012]. A phase front sensor (Phasics SID4) was placed directly in the beam after focus, close to the imaging plane of a deformable mirror (NightN, bimorph 40 element) which was used to tune out phase aberrations down to the limit imposed by shot to shot

fluctuations, which were at the λ/10 level RMS. Optimum results were achieved by using a circular aperture close to the focusing optic to clip out low amplitude portions of the beam. Unlike previous experiments[25] the aperture used here did not clip a significant fraction of the laser energy (≤10%), and was used principally to exclude the low-amplitude halo around the laser beam which could not be tuned effectively using the deformable mirror and phase front sensor. It also imposed a quasi-flat top near field distribution. The result was a high quality focal mode over the ~ 1.6 mm length of the plasma. Over 90% of the energy is in a Gaussian fit at focus, and over 75% at ± 0.8 mm from focus. This range corresponds to four times the focal depth estimated from the focal spot size, a range over which typical lasers used in LPA experiments exhibit multiple spots or rings. Temporally the laser had a 40 fs pulse length.

The symmetric laser mode improved propagation of the laser through the plasma. The plasma created by the laser was imaged using an interferometer. A nearly collimated plasma structure was seen, extending the full length of the 2mm gas target (Figure 10). This was confirmed by side-imaged Thomson scattering of the drive beam, which showed that the laser propagated without significant change in spot size. Visible transverse filamentation was eliminated, indicating that the laser pulse propagated without breakup as needed for efficient acceleration.

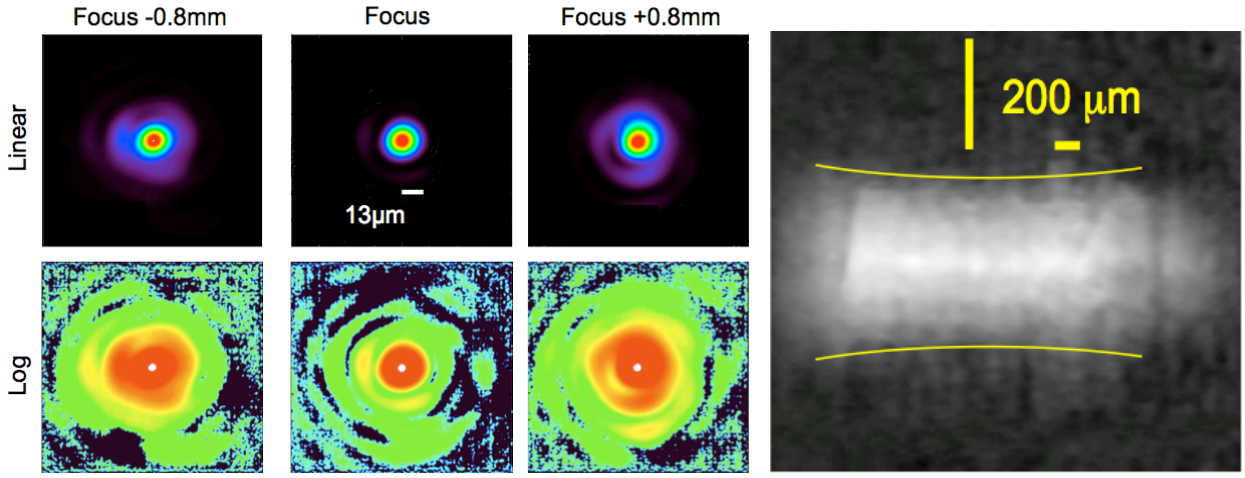

Figure 10. (left) Laser mode profiles for a 10 TW, 0.4 Joule laser after tuning to reduce laser aberrations and use of a deformable mirror to flatten the near field phase profile. Shown are images using linear (top) and log (bottom, with blue contour at 10^{-4} I_0) scales. The profile at the focal plane and at 0.8 mm on either side of focus are shown. (right) Interferometer image of the plasma created when the laser propagated through a gas jet, showing a collimated structure over 1.5 mm (note magnified vertical scale).

The collimated propagation observed is in contrast to previous data from the same laser system, prior to phase front tuning, which showed breakup of the laser pulse and rapid diffraction at similar plasma densities and lengths (above). However, even using the preformed guide, there was significantly more leakage of the laser outside the collimated structure in those experiments than in the present data. This indicates the effectiveness of the implemented laser mode control in establishing collimated propagation and lengthening acceleration length.

Laser guiding control produced record electron energies of 200-300 MeV from 10 TW laser power [MatlisAAC2012]. Electron beams were first produced using self-trapping [1] or downramp trapping [34] for comparison with colliding pulse results shown below. High energy and energy spreads as low as 2% were achieved (Figure 11), but energies were not tunable. The energies obtained are suitable for NRF and low energy radiography photon sources, and are comparable to other experiments using three to four times higher laser power. This can be compared to previous experiments using the same laser, which showed unstable beams with energies of ~30 MeV without preformed channel. Previous results with preformed guiding were limited to 86 MeV, confirming the effectiveness of the mode-controlled structure. Use of the lowest laser power is important for a transportable source. Simulations indicate that adding plasma channel preformed guiding may further increase energies, and an improved technique was developed to do this for future experiments.

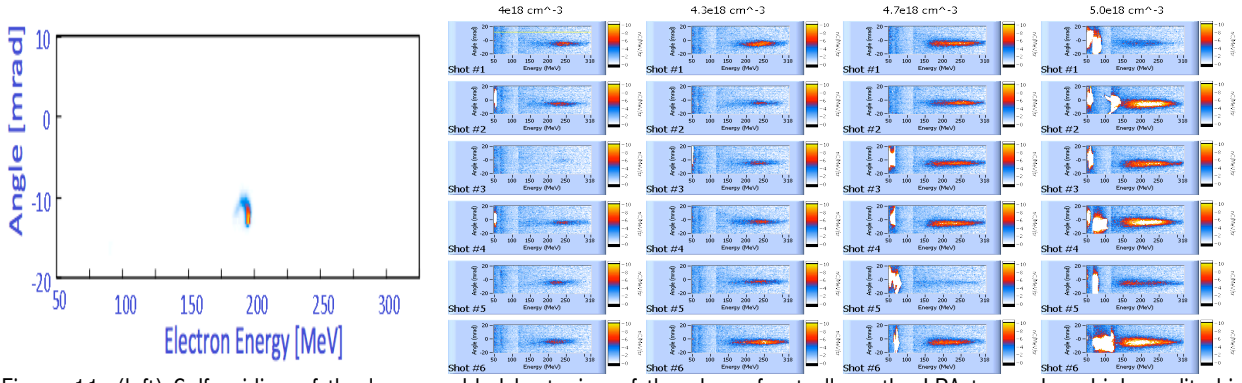

Figure 11. (left) Self-guiding of the laser enabled by tuning of the phase front allows the LPA to produce high quality high energy electron beams using self or downramp injection. (right) Stable operation was obtained, but beam energy was not tunable. The displayed variation of density turns trapping on or off but does not significantly change energy.

In the colliding pulse technique [26], the ponderomotive force of the beat between two nearly counter-propagating laser pulses is used to capture and inject particles into the accelerating phase of a wake which is operated below the trapping threshold. The strength of the beat is proportional to $a_0 \times a_1$ where $a_{0,1}$ are the normalized vector potentials of the two pulses. The simplest configuration uses a high intensity pulse to drive the wake, and a weaker colliding pulse to inject particles. The beat wave should capture particles in a region where there is accelerating field and where plasma density is nonzero. This motivates operation of the wake in a mildly nonlinear regime where the plasma is not fully blown out by the laser, and with plasma density such that the pulse length is in the range of one plasma period.

In past experiments on this laser[27], self guiding was not effective at colliding pulse relevant densities, near 10^{19}/cc. Those experiments mapped the longitudinal extent of the acceleration region by scanning the intersection of the colliding pulses, showing it to be limited to approximately 200 µm. This demonstrated injector operation but resulted in low energy electron production. Past experiments on 30 TW class lasers demonstrated high quality beams at 150-200 MeV [28], and experiments on other 10 TW class lasers produced energies up to 130 MeV with energy spreads near 10% FWHM [29].

In the project experiments [GeddesAAC2014], a second pulse split from the wake driver was used to implement colliding pulse controlled injection into the high energy structure described above. The colliding laser intersected the driver at 161 degrees. This is 19 degrees from counter-propagating, a large enough angle to avoid back-propagation of laser pulses which can damage the amplifier chains, but small enough that simulations indicate a negligible effect on the physics of the colliding pulse interaction. The collider had energy of up to 40 mJ in a spot near 10 µm FWHM, corresponding to $a_1 \sim 0.5 - 0.7$. This range was selected based on past experiments, simulations [CormierPRSTAB14] and theory [26]. The foci of the two pulses were overlapped in space and time as detailed in [27]. This included a top view camera to establish intersection in the horizontal plane and focal overlap, and transverse shadowgraphy to establish vertical alignment and timing. The accelerator was then operated at densities below the self trapping threshold and the colliding laser pulse was used to trigger injection.

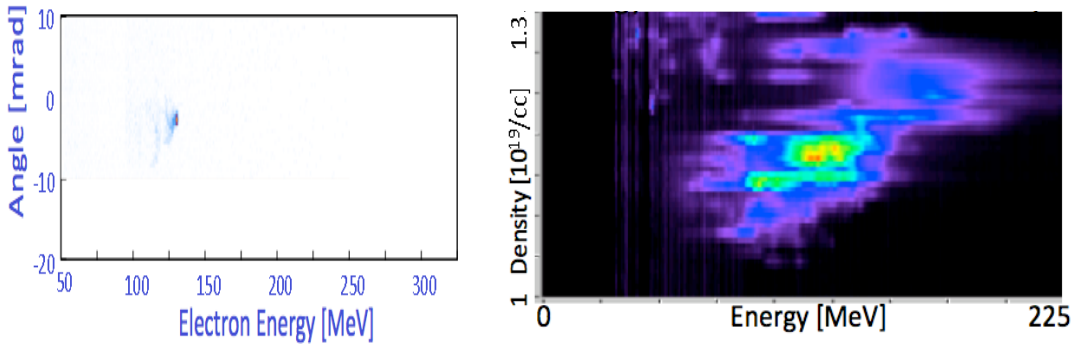

Figure 12. (left) The LPA produces high quality, high energy electron beams using colliding pulse injection. (center, showing averages over ~20shots per density) The energy of the beam is stable shot-to-shot and tunable with plasma density. Colliding pulse experiments developed techniques for stable laser overlap. Remaining jitter is much less than the laser spot size and will not disrupt scattering.

Colliding pulse injection into the controlled, high energy LPA structure established by laser phase front control (Figure 12) produced high quality beams, with energy spread <1.4% at 150-200 MeV from 10 TW. The energy spreads are equal to the lowest observed even on much larger lasers [30]. These energies can produce NRF-relevant photons using a frequency doubled scattering laser. Higher photon yield may be obtainable using the scattering laser fundamental frequency, which would require 300 MeV electrons and hence may require slightly higher laser power. The beam energy was tunable and controllable.

Injector methods were compared to establish suitability for a photon source. Self injected results described above are simpler and would be suitable for less stringent applications such as photofission and radiography, and for initial source experiments. The two-pulse colliding pulse electron beams are suitable for high quality photon sources relevant to NRF including 1% level energy spread, such that three pulse is not required at this stage. There is a broad parameter space in tuning charge, and beam quality, and hence it is likely that future work would lead to further gains. Three-pulse colliding pulse injection was demonstrated but has not so far produced higher quality beams than two pulse. Simulations indicate that for long term source development at < 1 % energy spread three pulse injection may be advantageous, but this requires shorter laser pulses or lower densities than the project work allowed.

The colliding pulse experiments developed techniques which will be required for future Thomson scattering, including stable timing and intersection of the laser pulses at fs and μm precision. Technology for aligning laser pulses includes use of side and top imagers and identification of scattering signatures that show intersection. These align the beams within the laser spot size. Automated beam pointing systems are in place which compensate thermal drifts. Remaining jitter in the beam lines is well below a laser spot size. This would be essential to a source in a vibration environment.

Related experiments also established that our LPA produces emittance (focusability) competitive with state of the art RF sources [PlateauPRL2012], as is necessary for high quality Thomson photon production. This was done using betatron radiation from the accelerator (Figure 13). Independent emittance measurements using another technique have derived a similar value [31]. The betatron mechanism is physically similar to Thomson scattering, and the developed detector and simulation techniques will support future Thomson scattering work.

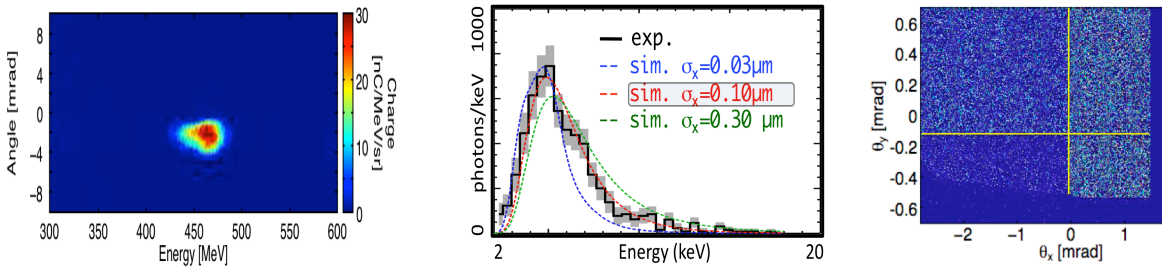

Figure 13. Emittance of a low energy spread 0.5 GeV LPA was inferred from simultaneous measurement of electron (left) and betatron X-ray spectra (center). Spectra were obtained by photon counting on a CCD (right), and confirmed by transmission a mosaic of different filters (yellow lines show borders).

These experiments indicate that compact, 10 TW class LPAs can produce high energy, high quality electron beams suitable for Thomson photon sources at NRF relevant energies, and that 40-100 TW class systems can produce energies required for Photofission and high energy radiography.

4: *Laser plasma accelerator-based electron beam disposal*

The deceleration of an electron beam in a second plasma-based structure is being studied to reduce background radiation production (Schematic, Figure 14). For a photon source this would dispose of the high energy electron beam after photons are produced, minimizing shielding requirements as needed for a transportable source [RykovanovJPB2014]. Experiments were conducted on deceleration, and preliminary designs were developed via simulations for a segmented plasma to compactly accomplish acceleration, scattering and deceleration in a single structure.

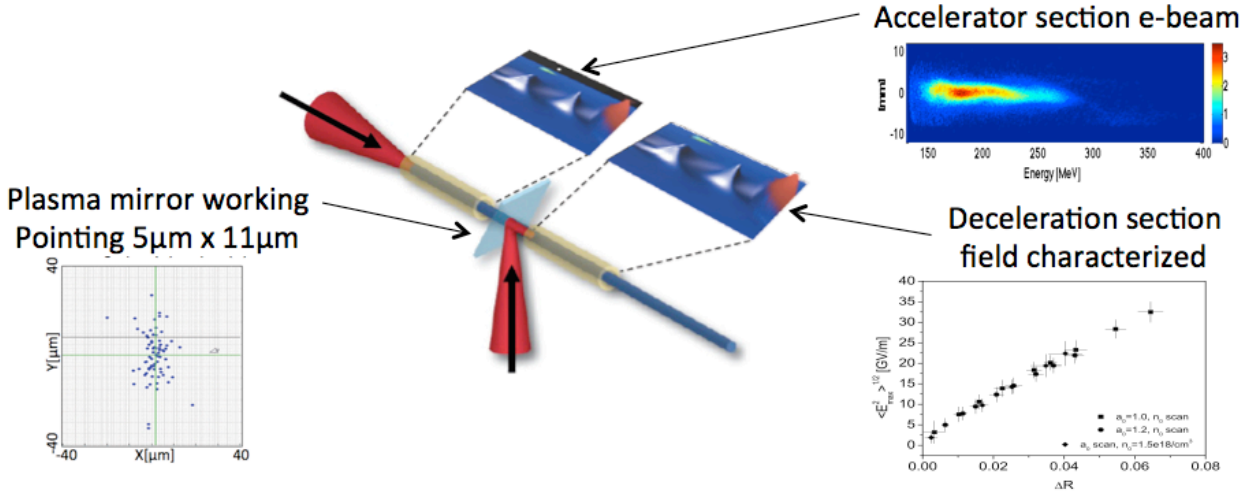

Figure 14. Deceleration experiments are in progress on a setup which accelerates an electron beam in one plasma, then decelerates it in a second.

The colliding pulse experiments described in Section 3 provided initial indications of deceleration in a single structure, by controlling injection point, acceleration length, and plasma density (Figure 15). In these experiments, the plasma density was changed, and a peak in energy was observed at a density near 1.2×10^{19}/cc. This is the density at which simulations indicate the electron beam dephases from the accelerating field, slipping into the decelerating phase of the wake. As anticipated, higher densities then lead to lower energies [GeddesAAC2014]. However, in these experiments the beam energy can only be measured at the output of the accelerator. Hence, to definitively evaluate deceleration it was important to use a setup in which electron beam energy can be measured after acceleration, then again after deceleration.

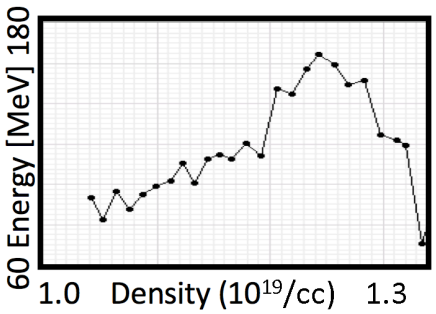

Figure 15. (left) Colliding pulse experiments demonstrate control of LPA energy. Peak energy is reached at the predicted density, indicating that the beam may be decelerating at higher densities

Deceleration experiments were conducted in a setup which allows acceleration in one structure, and deceleration in a second (Figure 14). These experiments were published in [SteinkeAAC2014] and are summarized here. The main tasks required to accomplish this were improvement of the first stage LPA stability, followed by careful alignment to the second stage. Previous work had already established the other elements necessary for deceleration. The presence and amplitude of the plasma decelerating field in the deceleration structure was demonstrated using optical diagnostics [32]. Coupling of the laser to the deceleration structure in a short distance (comparable to the LPA length) using a tape drive plasma mirror was also demonstrated [33].

The stability of the accelerated electron beam was improved to meet the high performance required for deceleration experiments. This was accomplished using plasma density gradients [34] to control injection (previously demonstrated on other LBNL systems). A very stable beam was produced over more than ten days of run time, limited by fluctuation of the laser front end, which is > 10 years old (Figure 16).

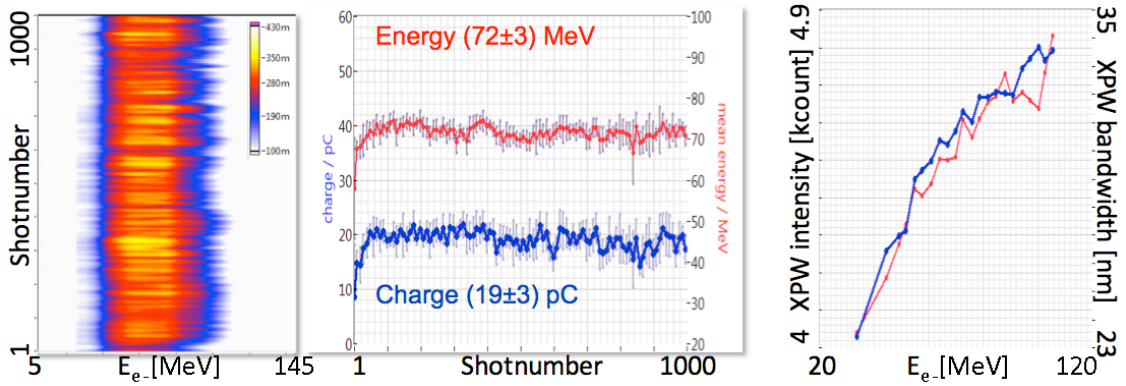

Figure 16. Stable first stage of deceleration experiment. (left) Energy spectra of 1000 consecutive shots on fixed color scale, showing reproducible beam. (center) Statistics show 5% percent level variation in energy, allowing precision deceleration experiment. (right) Remaining variation in energy is driven by variation in the laser front end.

The stable LPA electron beam developed was coupled to the second plasma stage. The second stage is a capillary discharge plasma in which the deceleration structure is powered by a second laser pulse sent into the capillary by a plasma mirror. The accelerated electron beam passes through this plasma mirror to enter the second stage. The delay of the drive laser pulse of the second plasma was varied with respect to that of the first LPA by an optical delay stage in the laser beamline of the first stage.

Experiments first demonstrated alignment of the accelerated beam through the narrow capillary (~4mrad acceptance). Focusing of the beam by the capillary discharge current [35] was then demonstrated, and used to refine alignment (Figure 17). This also demonstrates one method for implementing compact electron beam focusing optics for a future photon source where divergence control will be required to control source bandwidth. Focal length is at the cm scale, as opposed to meter scale for conventional magnetic quads.

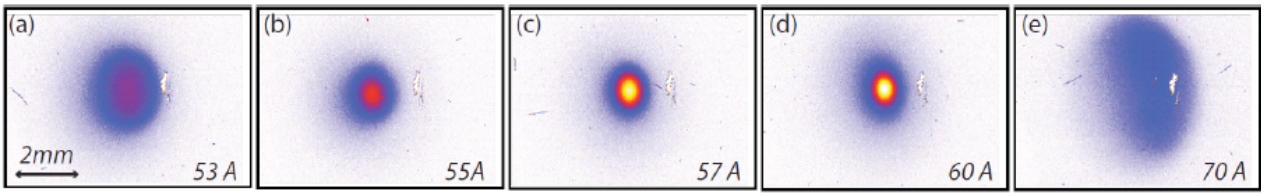

Figure 17. Electron beam profiles measured 1.7 m downstream of the exit of the capillary on the phosphor screen for different effective discharge currents ranging from 53 A in (a) to 70 A in (e). The mean electron beam energy was 100 MeV in all cases. The discharge current was varied by changing the arrival time of the electron beam with respect to the pulsed discharge which had a FWHM duration of 250 ns and a peak current of 300 A.

Electron spectra were recorded as a function of the delay between the two laser pulses driving the first- and the second stage (cf. Figure 18). This timing controls phasing in the structure, and hence deceleration. In the case of a negative delay, the first stage electrons propagate undistorted without the influence of the second laser pulse as expected. After the second laser pulse arrives (positive delay), the electron spectra are periodically modulated in energy with a modulation depth of ~30 MeV. The modulation period is consistent with the expected plasma wave period. The energy modulation observed is consistent with interaction over a distance of the Rayleigh length of the laser (1.5 mm). Such interaction over less than the full capillary length can occur due to mismatched focusing in the capillary, which is expected at these densities. Not all electrons coupled efficiently to the structure. Despite these limits, electrons are observed decelerated down to 50 MeV at timing near zero. Comparing this to the unperturbed beam shown at negative timing which has a minimum energy near 95 MeV indicates that some electrons were decelerated by approximately 50%. Improved deceleration should be accessible with improved guiding of the drive laser pulse at higher plasma density to increase decelerating field, better coupling of the electron beam to the second stage, and continuing to refine alignment.

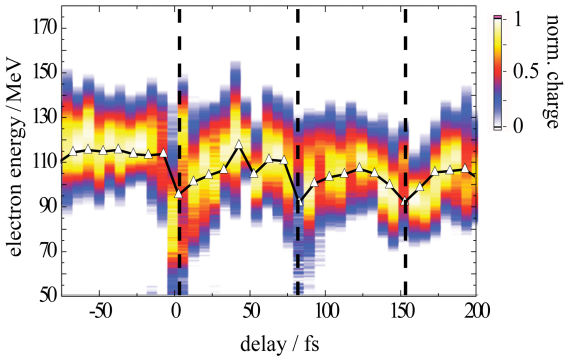

Figure 18. Injector beams probing the wakefield of the 2nd LPA stage: waterfall plot of normalized electron spectra shown vertically in color code. Each column represents a 5-shot averaged spectrum. The white triangles indicate the corresponding mean energy of the electron beam. Negative delay: The injector electrons arrive before the 2nd stage laser pulse and propagate undistorted. Positive delay: The 1st stage electrons are influenced by the presence of the wakefield generated by the 2nd stage laser pulse. The vertical, dashed lines emphasize the observed periodicity.

Simulations have demonstrated that coupling of the electron beam to the decelerating structure, and subsequent deceleration, can be controlled for improved performance. Coupling to increase the fraction of electrons effectively decelerated can be improved by tailoring the plasma exit density longitudinal profile as reported in FY13. Increased deceleration of each electron can then be achieved by improving guiding of the laser pulse through the second plasma.

Simulations were continued to improve deceleration and to develop concepts for an all in one, compact plasma structure that can accelerate, allow scattering, and then decelerate the electron beam. These were published in [VayNPNSNP2014, BonattoAAC2014]. For sources at the 10% photon bandwidth level, a single plasma channel can be used. This is because in an LPA the laser travels more slowly in the plasma than does the electron beam. The result is that the electron beam naturally slips forward in accelerator structure phase. The plasma structure has adjacent accelerating and focusing, then decelerating and focusing phases, and indeed the phase slippage (or dephasing) is a well known and primary limit on LPA energy. By lengthening the plasma, the electron beam naturally slips from accelerating to decelerating phase as it propagates. The result is a trajectory of energy versus propagation distance as shown in Figure 11. This structure achieves excellent deceleration of > 90%. The plasma channel can also guide the laser pulse to improve scattering photon yield as detailed under task 1. Simulations were conducted for a 500 MeV electron beam, and can be scaled to other energies such that similar deceleration performance is anticipated across the range of energies of interest for a photon source. Deceleration is limited because the electron beam develops a head to tail energy correlation, or chirp. This chirp can be removed, in principle allowing deceleration beyond 90%, by combining laser driven and passive (plasma only) stages, and simulations verified the effectiveness of such techniques. Such deceleration could allow a source to use significantly reduced radiation shielding while remaining within occupational dose limits. Further deceleration by tapering the plasma density, lighter duty factors, distance and other factors can further reduce bulk. Demonstration of deceleration after photon production will then be needed in integrated experiments.

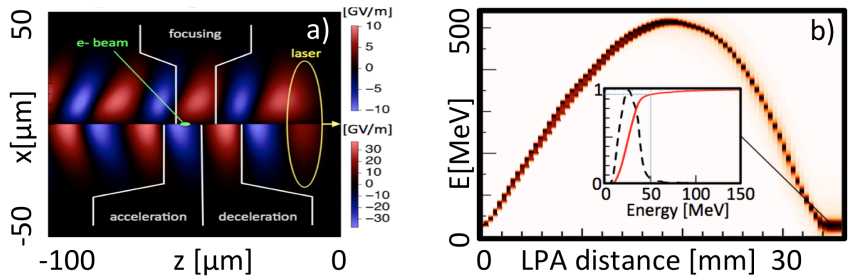

Figure 18. (a) Snapshot of the accelerating (z) and focusing (x) fields of an LPA plasma wave. With appropriate phasing of the injection of the electron beam (green), approximately half of a period is available for simultaneous guiding and acceleration, immediately followed by simultaneous guiding and deceleration of the electron beam. (b) Energy profile of the electron beam versus propagated distance in the plasma channel show that controlled deceleration can bring the beam down to ~ 10% of initial energy, greatly reducing shielding requirements. Photons would be produced at the center of the structure where energy is nearly constant (near ~18mm in this case).

Photon beam bandwidth in single plasma channels such as those shown in Figure 18 is currently limited to the 10 % level by the strong focusing forces of the LPA, which result in milliradian divergences for the state of the art emittances shown in Section 3. Several methods for compact electron refocusing to reduce this bandwidth are available, including tapered plasmas or plasma lenses. These can reduce divergence to allow bandwidths at or below the 1% level while maintaining compactness and compatibility with deceleration and with guiding of the scattering laser for efficient scattering. Advanced LPA injectors may also be possible to reduce emittance, which could provide a direct path to lower divergence and hence lower bandwidth. A paper detailing these approaches and their impact on Thomson source designs was published [RykovanovJPB2014]. This provides a path to a compact single plasma structure to accomplish acceleration, scattering, and deceleration. A concept of such a structure is shown in Figure 19.

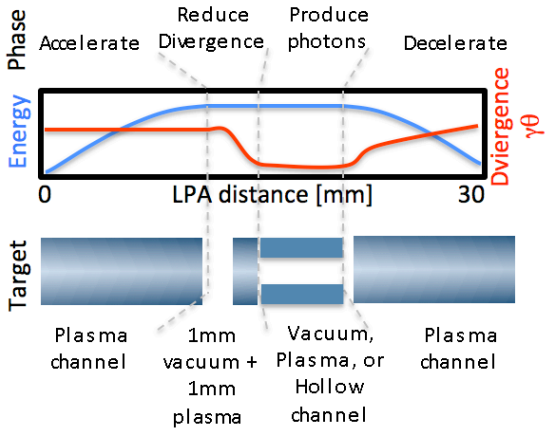

Figure 19. Longitudinally and transversely controlled plasma profiles are needed for future high flux, low bandwidth sources to incorporate LPA acceleration, divergence control, efficient scattering, and deceleration.

The experiments demonstrated that laser driven plasma structures can controllably decelerate electrons with similar high gradients to those long known to exist in plasma accelerators. Deceleration of some electrons by approximately 50 % was demonstrated. The simulations show that improved deceleration can be obtained by tuning coupling of the electrons to the decelerating wake, and guiding of the laser in the second stage to extend deceleration distance. Deceleration efficiencies above 90% have been observed in simulations, and techniques to obtain even greater deceleration by combining passive and active structures are being developed. A concept for an all in one plasma structure to accomplish acceleration, scattering, and deceleration was developed. These results indicate that plasma beam deceleration can reduce the beam energy after Thomson scattering photon production to significantly reduce required shielding and hence photon source size.

5. *Conclusion*

Project results indicate that Thomson scattering from LPA electron beams, with improvements realized under the project, can produce a high quality photon source from a laser of transportable size. They establish the elements required to enable a photon source demonstration. LPA performance was improved by controlling the accelerator structure and injector, producing record-setting beams and enabling use of smaller laser drivers. Energy spreads $\leq$ 1.4 %, emittances of 0.1 μm, and electron energies close to theoretical expectations were established. Performance of project experiments was limited by the stability of the laser system, parts of which are more than 15 years old. New, state of the art lasers are sufficient to allow a photon source demonstration near 10 Hz, which would integrate accelerator, scattering, and detection. Beam deceleration and disposal would then be added. Techniques such as guiding of the scattering laser and control of electron beam divergence then provide a path to a narrow bandwidth, high flux source using reasonable laser energies and beam currents. Pulsed photons beams can be characterized and used via detector concepts developed. Experiments also show deceleration is achievable, and simulations indicate that it can be effective enough to enable compact shielding. The kHz laser technology to enable anticipated scan rates is under rapid development, led by other funding agencies and by commercial companies.

6. *Acknowledgements and notices*

This project was supported by the U.S. Dept. of Energy National Nuclear Security administration Defense Nuclear Nonproliferation R&D (NA-22). The work was additionally supported by the Office of Science Office of High Energy Physics, under Contract No. DE-AC02-05CH11231. The simulations used the computational facilities at the National Energy Research Scientific Computing Center, a DOE Office of Science User Facility supported by the Office of Science of the U.S. Department of Energy under Contract No. DE-AC02-05CH11231. The authors gratefully acknowledge technical support from Dave Evans, Mark Kirkpatrick, Art Magana, Greg Mannino, Joe Riley, Ken Sihler, Ohmar Sowle, Tyler Sipla, Don Syversrud, and Nathan Ybarrolaza. We thank Maurice Garcia-Sciveres, Guinevere Shaw, Brian Shaw, Jeroen van Tilborg, Max Zolotorev, Carlo Benedetti, Min Chen, Stepan Bulanov, Mike Fisher, Estelle Cormier-Michel, David Bruhwiler and Francesco Rossi for their contributions and discussions.

Project publications:

- G. R. Plateau, C. G. R. Geddes, D. B. Thorn, M. Chen, C. Benedetti, E. Esarey, A.J. Gonsalves, N.H. Matlis, K. Nakamura, C.B. Schroeder, S. Shiraishi, T. Sokollik, J. van Tilborg, Cs. Toth, S. Trotsenko, T.S. Kim, M. Battaglia, Th. Stoehlker, and W. P. Leemans, "Low-emittance electron bunches from a laser-plasma accelerator measured using single-shot X-ray spectroscopy," PRL 109, 064802 (2012).
- S. G. Rykovanov, M. Chen, C. G. R. Geddes, C. B. Schroeder, E. Esarey and W. P. Leemans, "Virtual Detector of Synchrotron Radiation (VDSR) - the C++parallel code for particle tracking and radiation calculation," accepted to Proceedings of the Advanced Accelerator Concepts Workshop 2012.
- M. Chen, C.G.R. Geddes, E. Esarey, C.B. Schroeder, S.S. Bulanov, C. Benedetti, L.L. Yu, S. Rykovanov, W.P. Leemans, E. Cormier-Michel and David L. Bruhwiler, "Using transverse colliding-pulse injection to obtain electron beams with small emittance in a laser-plasma accelerator," accepted to Proceedings of the Advanced Accelerator Concepts Workshop 2012.
- C. G. R. Geddes, G. R. Plateau, D. B. Thorn, M. Chen, C. Benedetti, E. Esarey, A. J. Gonsalves, N. H. Matlis, K. Nakamura, S. Rykovanov, C. B. Schroeder, S. Shiraishi, T. Sokollik, J. van Tilborg, Cs. Toth, S. Trotsenko, T. S. Kim, M. Battaglia, Th. Stöhlker, and W. P. Leemans, "Low-emittance electron bunches from a laser- plasma accelerator measured using single-shot X- ray spectroscopy," accepted to Proceedings of the Advanced Accelerator Concepts Workshop 2012.
- N.H. Matlis, C.G.R. Geddes, G.R. Plateau, E. Esarey, C. Schroeder, D.L. Bruhwiler, E. Cormier-Michel, M. Chen, L. Yu, and W.P. Leemans, "Controlling Electron Injection in Laser Plasma Accelerators Using Multiple Pulses," accepted to Proceedings of the Advanced Accelerator Concepts Workshop 2012.
- M. Chen, E. et al., "Modeling classical and quantum radiation from laser-plasma accelerators," Phys. Rev. Special Topics -AB, V. 16, 030701 (2013).
- M. Chen, E. Esarey, C. G. R. Geddes, E. Cormier-Michel, C. B. Schroeder, S. S. Bulanov, C. Benedetti, L. L. Yu, S. Rykovanov, D. L. Bruhwiler, and W. P. Leemans, "Electron injection and emittance control by transverse colliding pulses in a laser-plasma accelerator," Phys. Rev. ST Accel. Beams 17, 051303
- S.G. Rykovanov, C.G.R. Geddes, J.-L. Vay, C.B. Schroeder, E. Esarey, W.P. Leemans, "Quasi-monoenergetic femtosecond photon sources from Thomson Scattering using laser plasma accelerators and plasma channels," submitted to J. Phys B 2014; arXiv:1406.1832.
- J.-L. Vay, C. G. R. Geddes, S. G. Rykovanov, C. B. Schroeder, E. Esarey and W. P. Leemans, "L aser-driven plasma deceleration of electron beams for compact photon sources," submitted to the proceedings of the Nuclear Physics and Photon-ray sources for Nuclear Security and Nonproliferation conference, Tokai-Mura Japan, January 2014.
- S. Steinke, N. H. Matlis, J. van Tilborg, B. H. Shaw, C. G. R. Geddes, A. J. Gonsalves, K. Nakamura, D. E. Mittelberger, J. Daniels, A. D. Roberts, T. Sokollik, S. Shiraishi, J. -L. Vay, E. Esarey, C. B. Schroeder, C. Benedetti, C. Toth and W. P. Leemans, "Staged Acceleration Experiments," proceedings of the Advanced Accelerator Concepts Workshop, 2014.
- A. Bonatto, C. B. Schroeder, J.-L. Vay, C. R. Geddes, C. Benedetti, E. Esarey and W. P. Leemans, "Compact disposal of high-energy electron beams using passive or laser-driven plasma decelerating stage," proceedings of the Advanced Accelerator Concepts Workshop, 2014.
- C.G.R. Geddes, N.H. Matlis, S. Steinke, E. Esarey, K. Nakamura, G.R. Plateau, C.B. Schroeder, Cs. Toth, W.P. Leemans, 'High energy, low energy spread electron bunches produced via colliding pulse injection," proceedings of the Advanced Accelerator Concepts Workshop, 2014.
- E. Cormier-Michel, V. H. Ranjbar, D. L. Bruhwiler, J. R. Cary, M. Chen, C. G. R. Geddes, G. R. Plateau, N. H. Matlis, and W. P. Leemans, "Design principles for high quality electron beams via colliding pulses in laser plasma accelerators," Phys. Rev. ST Accel. Beams 17, 091301 (2014).
- C.G.R. Geddes, N.H. Matlis, S. Steinke, E. Esarey, D.E. Mittelberger, S. Rykovanov, C.B. Schroeder, Cs. Toth, J.-L Vay, W.P. Leemans, "Laser Technology for Thomson MeV Photon Sources Based on Laser-Plasma Accelerators," proceedings of the Advanced Accelerator Concepts Workshop, 2014.
- C.G.R. Geddes , S. Rykovanov, N.H. Matlis, S. Steinke, J.-L. Vay, E.H. Esarey , B. Ludewigt , K. Nakamura , B.J. Quiter , C.B. Schroeder , C.Toth, W.P. Leemans, "Nuclear detection and characterization with laser-plasma accelerator driven compact quasi-monoenergetic photon sources," proceedings of the Conference on Applications of Accelerators in Research and Industry, 2014.
- N.H. Matlis, A.J. Gonsalves, S. Steinke, J. van Tilborg, C.G.R. Geddes, B. Shaw and W.P. Leemans, "Gas Dynamics in Longitudinally-structured LPA Targets," proc. Advanced Accelerator Concepts Workshop, 2014.

References:

[1] T. Tajima and J. Dawson, Phys. Rev. Lett. **43**, 267 (1979). W.P. Leemans and E. Esarey, Physics Today March p44 (2009). E. Esarey et al, RMP **81**, 1229 (2009).
[2] M. Chen, E. Esarey, C. G. R. Geddes, et al. Phys. Rev. Special Topics -AB, V. 16, 030701 (2013)
[3] J. Pruet, et al., Journal Of Applied Physics 99, 123102 (2006).
[4] R. Hajima, et al., Nuclear Instruments and Methods in Physics Research A v 608, pp557, (2009).
[5] B.J. Quiter et al, J. Appl. Phys. **103**, 064910 (2008).
[6] M. Johnson, et al., AIP Conference Proceedings, Vol. 1336 Issue 1, p590 (2011).
[7] Runkle, R. C., Chichester, D. L., and Thompson, S. J., Nucl. Inst. Meth. Phys. Res. A. 663 75-95 (2012).
[8] W.P. Leemans, et al., IEEE Trans. Plasma Sci., vol. 33, no. 1, pp. 8-22 (2005).
[9] H.R. Weller et al, Proc. Part. Nucl. Phys. 62 p. 257 (2009).
[10] F. Albert et al., Phys. Rev. ST-AB, **13**, 070704 (2010)
[11] O. Teşileanu, et al., Journal of Physics:ConferenceSeries 420 (2013).
[12] ASTA: http://asta.fnal.gov/files/ASTA_Proposal_October_2013.pdf
[13] FACETII: https://portal.slac.stanford.edu/sites/ard_public/facet/Documents/FACET-II%20Proposal%20v6.pdf
[14] ATF: http://www.bnl.gov/atf/
[15] W.P. Leemans et al., Phys. Rev. Lett. 77, p. 4182 (1996).
[16] A. Jochmann, et al., PRL 111, 114803 (2013).
[17] C.G.R. Geddes, et al., Physics of Plasmas, V 10, no. 8, pp.3422-25 (2003).
[18] H. Schwoerer, et al., Phys. Rev. Lett, **96**, 104802 (2006)
[19] K.T. Phuoc et al., Nat. Photonics **6**, 308 (2012). Also U.M.
[20] S.Y. Chen, et al., Phys. Rev. Lett. **110**, 155003 (2013). Similar exp. at MPQ.
[21] C. B. Schroeder et al., Phys. Plasmas **20**, 080701 (2013).
[22] I. Ghebregziabher, et al., Phys. Rev. Spec. Top. - Accel. Beams **16**, 030705 (2013).
[23]ICFA beam dynamics newsletter #56 (2011), http://www-bd.fnal.gov/icfabd/Newsletter56.pdf.
[24] C.G.R. Geddes, et al., Nature, V 438, pp. 538-41 (2004).
[25] T.P.A Ibbotson et al., New J. Phys **12** 045008 (2010).
[26] E. Esarey et al., Phys. Rev. Letters **79**, 2682 (1997). G. Fubiani et al., Phys. Rev. E 70, 016402 (2004). H. Kotaki, Phys. Plasmas 11, 6, 3296 (2004)
[27] C. Toth et al., Proc. Particle Accel Conference, 2975-77 (2007). C.G.R. Geddes et al., Proc. Particle Accel. Conf. MOP123 (2011).
[28] J. Faure et al., Nature **444**, 737-739 (2006).
[29] H. Kotaki et al., Phys. Rev. Lett. **103**, 194803 (2009).
[30] R. Weingartner et al., Phys. Rev. ST-AB 15, 111302(2012).
[31] C. Rechatin et al., Phys. Rev. Lett. 102, 164801 (2009).
[32] S. Shiraishi, et al., Physics of Plasmas, 20, 063103 (2013).
[33] T. Sokollik, et al., AIP Conference Proceedings, 1299, 233–7 (2010).
[34] S. Bulanov et al., Physical Review E, 58, R5257–R5260 (1998). C.G.R. Geddes et al., Physical Review Letters, 100, 215004 (2008).
[35] E. B. Forsyth, et al., J, Ieee Transactions on Nuclear Science, NS12, 872–876 (1965).